ENCLOSURE 2

TENNESSEE VALLEY AUTHORITY
BROWNS FERRY NUCLEAR PLANT (BFN)
UNITS 1, 2, AND 3

TECHNICAL SPECIFICATIONS (TS) CHANGES TS-431 AND TS-418
EXTENDED POWER UPRATE (EPU)

CDI REPORT NO. 08-05NP, "ACOUSTIC AND LOW FREQUENCY HYDRODYNAMIC LOADS AT CLTP POWER LEVEL ON BROWNS FERRY NUCLEAR UNIT 2 STEAM DRYER TO 250 HZ"

(NON-PROPRIETARY VERSION)

Attached is the non-proprietary version of CDI Report No. 08-05, "Acoustic and Low Frequency Hydrodynamic Loads at CLTP Power Level on Browns Ferry Nuclear Unit 2 Steam Dryer to 250 Hz."

C.D.I. Report No. 08-05NP

Acoustic and Low Frequency Hydrodynamic Loads at CLTP Power Level on Browns Ferry Nuclear Unit 2 Steam Dryer to 250 Hz

Revision 3

Prepared by

Continuum Dynamics, Inc.
34 Lexington Avenue
Ewing, NJ 08618

Prepared under Purchase Order No. 00053157 for

TVA / Browns Ferry Nuclear Plant
Nuclear Plant Road, P. O. Box 2000 PAB-2M
Decatur, AL 35609

Approved by

Alan J. Bilanin

Prepared by

Milton E. Teske

October 2008

Executive Summary

Measured strain gage time-history data in the four main steam lines at Browns Ferry Nuclear Unit 2 (BFN2) were processed by a dynamic model of the steam delivery system to predict loads on the full-scale steam dryer. These measured data were first converted to pressures, then positioned on the four main steam lines and used to extract acoustic sources in the system. A validated acoustic circuit methodology was used to predict the fluctuating pressures anticipated across components of the steam dryer in the reactor vessel. The acoustic circuit methodology included a low frequency hydrodynamic contribution, in addition to an acoustic contribution at all frequencies. This pressure loading was then provided for structural analysis to assess the structural adequacy of the steam dryer in BFN2.

This effort provides BFN2 with a dryer dynamic load definition that comes directly from measured BFN2 full-scale data and the application of a validated acoustic circuit methodology, at a power level where data were acquired.

Table of Contents

1. Introduction

In Spring 2005 Exelon installed new stream dryers into Quad Cities Unit 2 (QC2) and Quad Cities Unit 1. This replacement design, developed by General Electric, sought to improve dryer performance and overcome structural inadequacies identified on the original dryers, which had been in place for the last 30 years. As a means for confirming the adequacy of the steam dryer, the QC2 replacement dryer was instrumented with pressure sensors at 27 locations. These pressures formed the set of data used to validate the predictions of an acoustic circuit methodology under development by Continuum Dynamics, Inc. (C.D.I.) for several years [1]. One of the results of this benchmark exercise [2] confirmed the predictive ability of the acoustic circuit methodology for pressure loading across the dryer, with the inclusion of a low frequency hydrodynamic load. This methodology, validated against the Exelon full-scale data and identified as the Modified Bounding Pressure model, is used in the effort discussed herein.

This report applies this validated methodology to the Browns Ferry Nuclear Unit 2 (BFN2) steam dryer and main steam line geometry. Strain gage data obtained from the four main steam lines were used to predict pressure levels on the BFN2 full-scale dryer at Current Licensed Thermal Power (CLTP).

2. Modeling Considerations

The acoustic circuit analysis of the BFN2 steam supply system is broken into two distinct analyses: a Helmholtz solution within the steam dome and an acoustic circuit analysis in the main steam lines. This section of the report highlights the two approaches taken here. These analyses are then coupled for an integrated solution.

2.1 Helmholtz Analysis

A cross-section of the steam dome (and steam dryer) is shown below in Figure 2.1, with BFN2 dimensions as shown [3]. The complex three-dimensional geometry is rendered onto a uniformly-spaced rectangular grid (with mesh spacing of approximately 1.5 inches to accommodate frequency from 0 to 250 Hz in full scale), and a solution, over the frequency range of interest, is obtained for the Helmholtz equation

$$\frac{\partial^2 P}{\partial x^2}+\frac{\partial^2 P}{\partial y^2}+\frac{\partial^2 P}{\partial z^2}+\frac{\omega^2}{a^2}P=\nabla^2 P+\frac{\omega^2}{a^2}P=0$$

where P is the pressure at a grid point, ω is frequency, and a is acoustic speed in steam.

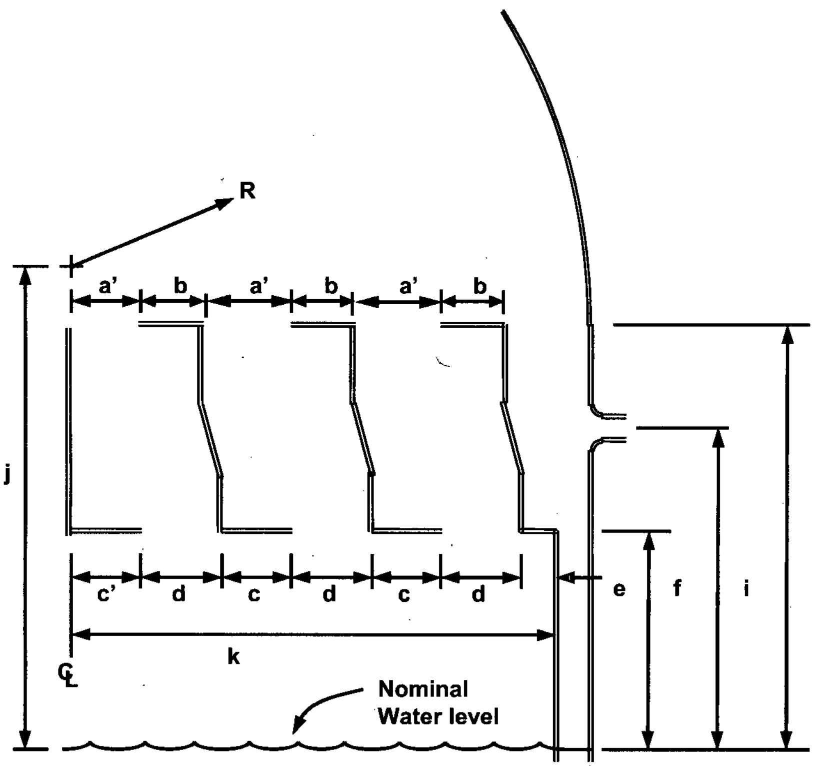

Figure 2.1. Cross-sectional description of the steam dome and dryer, with the BFN2 dimensions of a' = 16.0 in, b = 16.0 in, c' = 24.0 in, c = 14.5 in, d = 17.5 in, e = 15.5 in, f = 74.0 in, g = 163.0 in, i = 97.5 in, j = 189.0 in, k = 121.0 in, and R = 125.7 in (dimensions deduced from [3] to within 1.5 inches).

This equation is solved for incremental frequencies from 0 to 250 Hz (full scale), subject to the boundary conditions

$$\frac{dP}{dn} = 0$$

normal to all solid surfaces (the steam dome wall and interior and exterior surfaces of the dryer),

$$\frac{dP}{dn} \propto \frac{i\omega}{a} P$$

normal to the nominal water level surface, and unit pressure applied to one inlet to a main steam line and zero applied to the other three.

2.2 Acoustic Circuit Analysis

The Helmholtz solution within the steam dome is coupled to an acoustic circuit solution in the main steam lines. Pulsation in a single-phase compressible medium, where acoustic wavelengths are long compared to transverse dimensions (directions perpendicular to the primary flow directions), lend themselves to application of the acoustic circuit methodology. If the analysis is restricted to frequencies below 250 Hz, acoustic wavelengths are approximately 8 feet in length and wavelengths are therefore long compared to most components of interest, such as branch junctions.

Acoustic circuit analysis divides the main steam lines into elements which are each characterized, as sketched in Figure 2.2, by a length L, a cross-sectional area A, a fluid mean density $\bar{\rho}$, a fluid mean flow velocity $\bar{U}$, and a fluid mean acoustic speed $\bar{a}$.

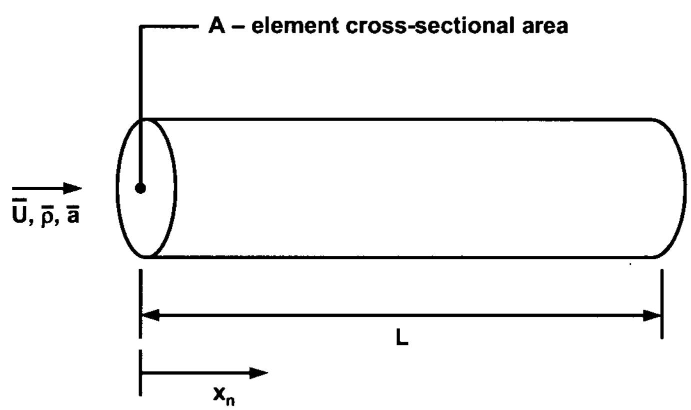

Figure 2.2. Schematic of an element in the acoustic circuit analysis, with length L and cross-sectional area A.

Application of acoustic circuit methodology generates solutions for the fluctuating pressure P_n and velocity u_n in the n^{th} element of the form

$$P_n = \left[A_n e^{ik_{1n}x_n} + B_n e^{ik_{2n}x_n}\right] e^{i\omega t}$$

$$u_n = -\frac{1}{\rho \bar{a}^2}\left[\frac{\left(\omega + \overline{U}_n k_{1n}\right)}{k_{1n}} A_n e^{ik_{1n}x_n} + \frac{\left(\omega + \overline{U}_n k_{2n}\right)}{k_{2n}} B_n e^{ik_{2n}x_n}\right] e^{i\omega t}$$

where harmonic time dependence of the form $e^{i\omega t}$ has been assumed. The wave numbers k_{1n} and k_{2n} are the two complex roots of the equation

$$k_n^{\,2} + i\frac{f_n\left|\overline{U}_n\right|}{D_n \bar{a}^{-2}}\left(\omega + \overline{U}_n k_n\right) - \frac{1}{\bar{a}^{-2}}\left(\omega + \overline{U}_n k_n\right)^2 = 0$$

where f_n is the pipe friction factor for element n, D_n is the hydrodynamic diameter for element n, and $i = \sqrt{-1}$. A_n and B_n are complex constants which are a function of frequency and are determined by satisfying continuity of pressure and mass conservation at element junctions.

The solution for pressure and velocity in the main steam lines is coupled to the Helmholtz solution in the steam dome, to predict the pressure loading on the steam dryer.

The main steam line piping geometry is summarized in Table 2.1.

Table 2.1. Main steam line lengths at BFN2. Main steam line diameter is 26 inch (ID = 24.0 in).

Main Steam Line	Length to First Strain Gage Measurement (ft)	Length to Second Strain Gage Measurement (ft)
A	9.5	38.1
B	9.5	39.8
C	9.5	39.5
D	9.5	38.2

2.3 Low Frequency Contribution

[[

(3)]]

3. Input Pressure Data

Strain gages were mounted on the four main steam lines of BFN2. Four data sets were examined in this analysis. The first data set recorded the strain at Current Licensed Thermal Power (100% power level or CLTP), the second data set recorded the strain at near-zero voltage on the strain gages (EIC noise) at CLTP, the third data set recorded the strain at 5% power level, and the fourth data set recorded the strain at near-zero voltage on the strain gages (EIC noise) at 5% power level. The data were provided in the following files:

Data File Name	Power Level	Voltage
20061128172906	100%	10.0 V
20061128172419	100%	0.01 V (EIC)
20080922060030	5%	10.0 V
20080922055401	5%	0.01 V (EIC)

The strain gage signals were converted to pressures by the use of the conversion factors provided in [4] and summarized in Table 3.1. Exclusion frequencies were used to remove extraneous signals, as also identified in [4] and subsequent emails, and summarized in Tables 3.2 and 3.3. The electrical noise was removed by applying the function

$$P_S(\omega) = P_{SN}(\omega)\left[1 - \left|\frac{P_N(\omega)}{P_{SN}(\omega)}\right|\right]$$

where $P_S(\omega)$ is the CLTP signal $P_{SN}(\omega)$ corrected for electrical noise $P_N(\omega)$, computed as a function of frequency ω, and $|P_N(\omega)/P_{SN}(\omega)|$ can be no larger than 1.0. These signals were further processed by the coherence factor and mean filtering as described in [2]. Coherence at CLTP and Low Power conditions is shown in Figure 3.1.

The resulting main steam line pressure signals may be represented in two ways, by their minimum and maximum pressure levels, and by their PSDs. Table 3.4 provides the pressure level information, after removal of EIC and exclusion filtering, while Figures 3.2 to 3.5 compare the frequency content at the eight measurement locations. The frequency content around 218 Hz has been removed from the signals plotted here, in anticipation of the use of inserts in the blank standpipes on main steam lines A and D [5] to mitigate this load.

Note from Table 3.1 that the lower main steam line D data are not available for the 5% power level. As the missing data are anticipated to be similar to the main steam line A data, the main steam line A data were substituted for both the upper and lower main steam line D data, with the upper main steam line A data scaled by the ratio of the magnitude of the upper main steam line D data to the upper main steam line A data. In this way, phasing between the upper and lower main steam line locations on main steam line D was preserved.

Table 3.1. Conversion factors from strain to pressure [4]. Channels are averaged to give the average strain; asterisked sensors (*) indicate that the sensor was inoperative during collection of the 5% power level data.

	Strain to Pressure (psid/μstrain)	Channel Number	Channel Number	Channel Number	Channel Number
MSL A Upper	3.088	1	2*	3	4
MSL A Lower	2.987	5	6	7	8
MSL B Upper	3.070	9	10	11	12
MSL B Lower	3.040	13	14	15	16
MSL C Upper	3.008	17	18	19	20
MSL C Lower	3.041	21	22	23	24
MSL D Upper	3.017	25	26	27	28
MSL D Lower	3.022	29*	30*	31*	32*

Table 3.2. Exclusion frequencies for BFN2 strain gage data, as suggested in [4]. VFD = variable frequency drive, Low Power. Recirc = recirculation pumps

Low Power Frequency Interval (Hz)	Exclusion Cause
0 – 2	Mean
59.8 – 60.2	Line Noise
119.8 – 120.2	Line Noise
179.5 – 180.5	Line Noise
239.7 – 240.2	Line Noise
16.0 Intervals	VFD (15 exclusions)

Table 3.3. Exclusion frequencies for BFN2 strain gage data, as suggested in [4]. VFD = variable frequency drive, CLTP. Recirc = recirculation pumps

CLTP Frequency Interval (Hz)	Exclusion Cause
0 – 2	Mean
59.9 – 60.1	Line Noise
119.9 – 120.1	Line Noise
179.9 – 180.1	Line Noise
239.9 – 240.1	Line Noise
44.7 – 46.0	VFD (1x)
90.8 – 91.0	VFD (2x)
136.1 – 136.5	VFD (3x)
181.6 – 181.8	VFD (4x)
227.1 – 227.4	VFD (5x)
112.7 – 113.2	Recirc Pump A Speed (5x)
110.4 – 111.7	Recirc Pump B Speed (5x)
218.6 – 220.2	Standpipe Excitation

Table 3.4. Main steam line (MSL) pressure levels in BFN2: CLTP.

	Minimum Pressure (psid)	Maximum Pressure (psid)	RMS Pressure (psid)
MSL A Upper	-2.91	2.09	0.51
MSL A Lower	-1.86	2.06	0.48
MSL B Upper	-1.79	1.62	0.41
MSL B Lower	-2.49	2.12	0.49
MSL C Upper	-2.33	2.19	0.55
MSL C Lower	-3.25	2.40	0.58
MSL D Upper	-1.95	2.08	0.48
MSL D Lower	-1.65	2.21	0.43

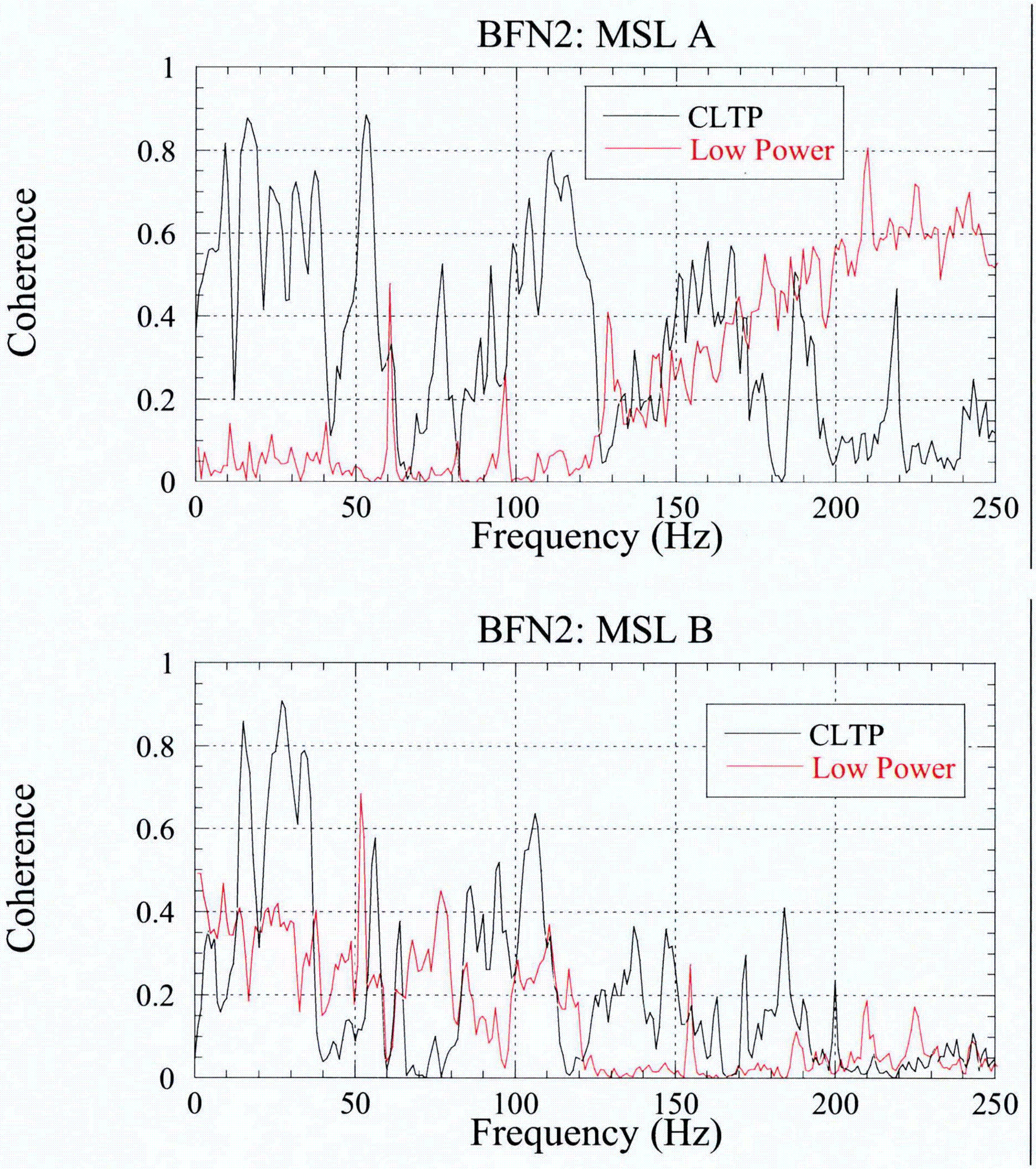

Figure 3.1a. Coherence between the upper and lower strain gage readings at BFN2: main steam line A (top); main steam line B (bottom); for CLTP (black curves) and Low Power (red curves).

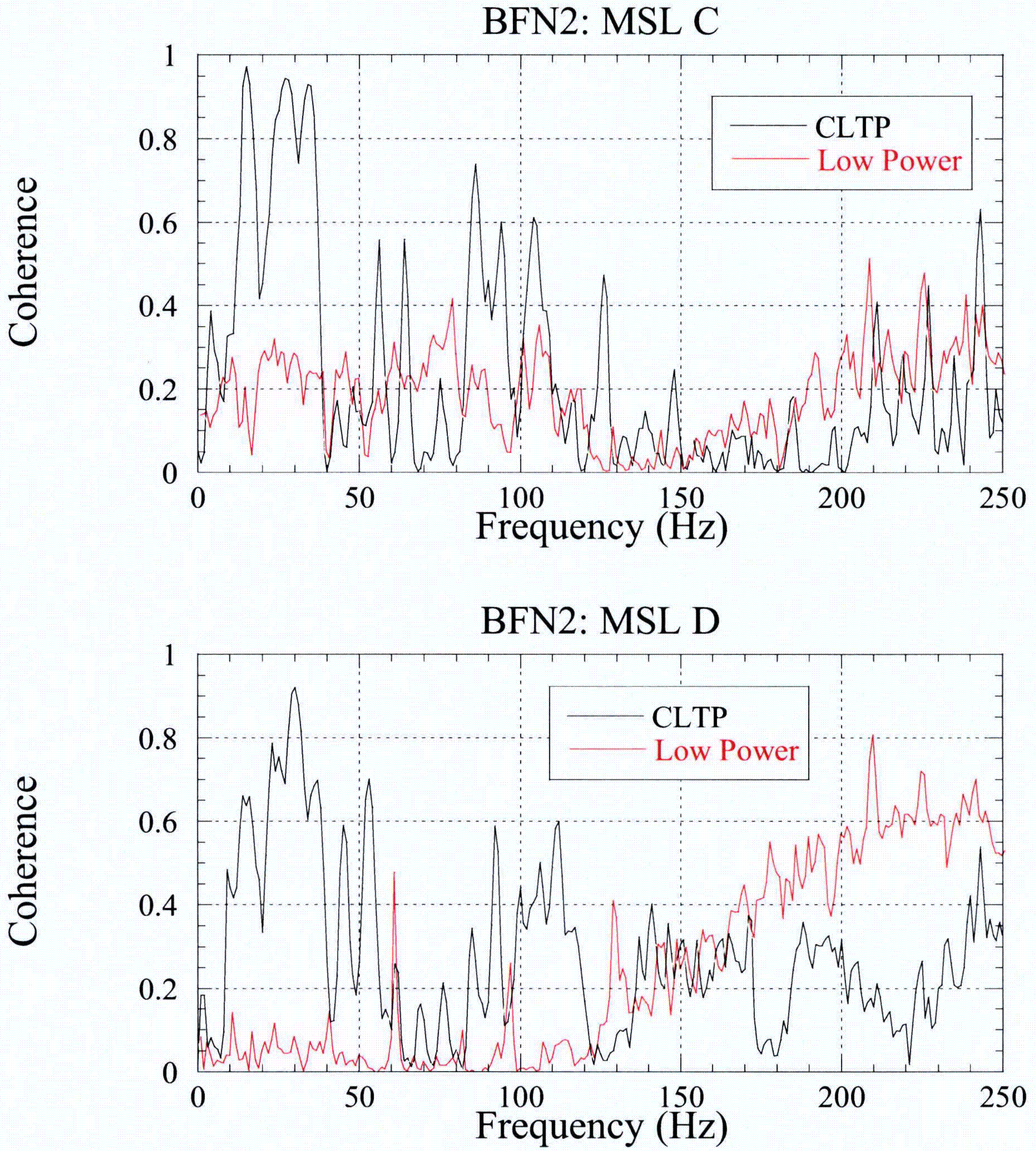

Figure 3.1b. Coherence between the upper and lower strain gage readings at BFN2: main steam line C (top); main steam line D (bottom); for CLTP (black curves) and Low Power (red curves).

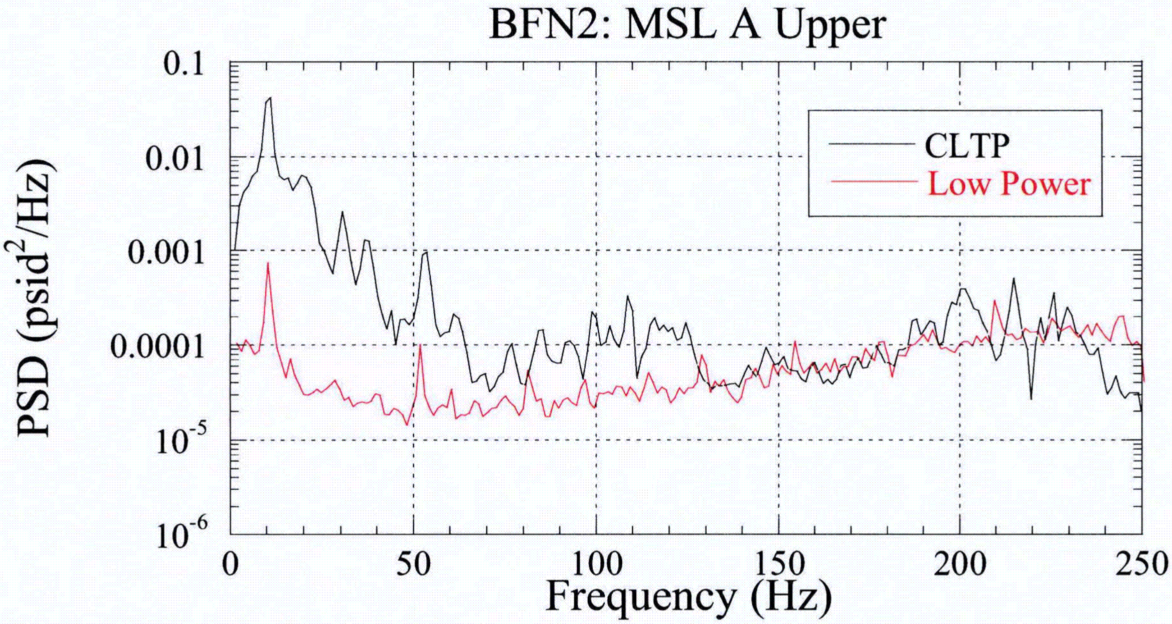

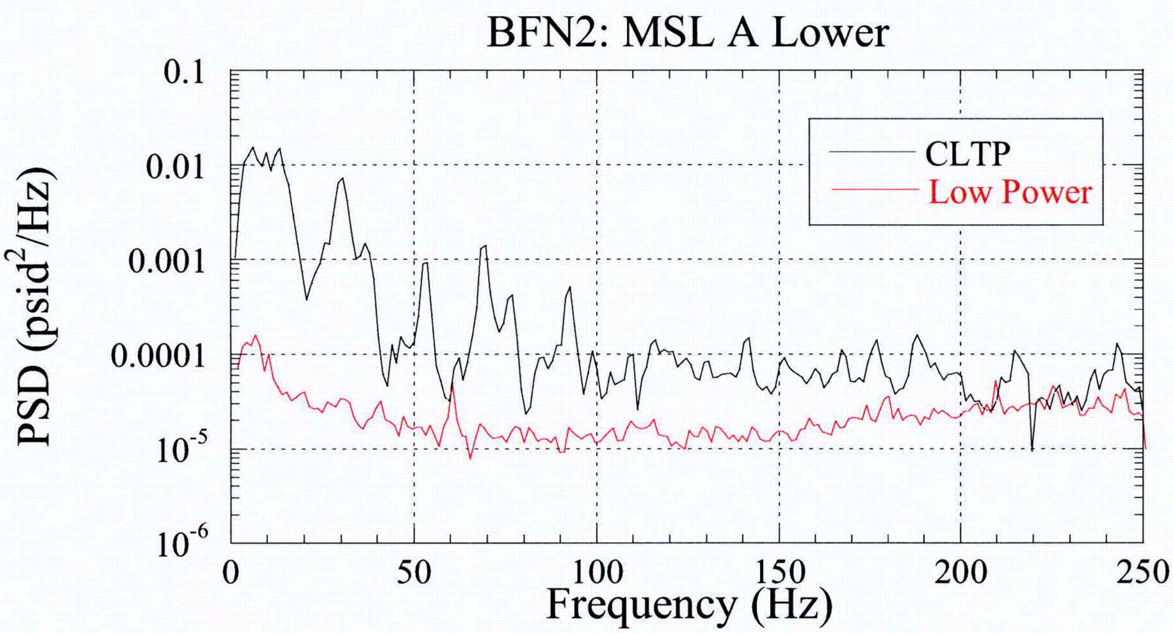

Figure 3.2. PSD comparison of pressure measurements on main steam line A at strain gage locations upper (top) and lower (bottom), for CLTP (black curves) and Low Power (red curves).

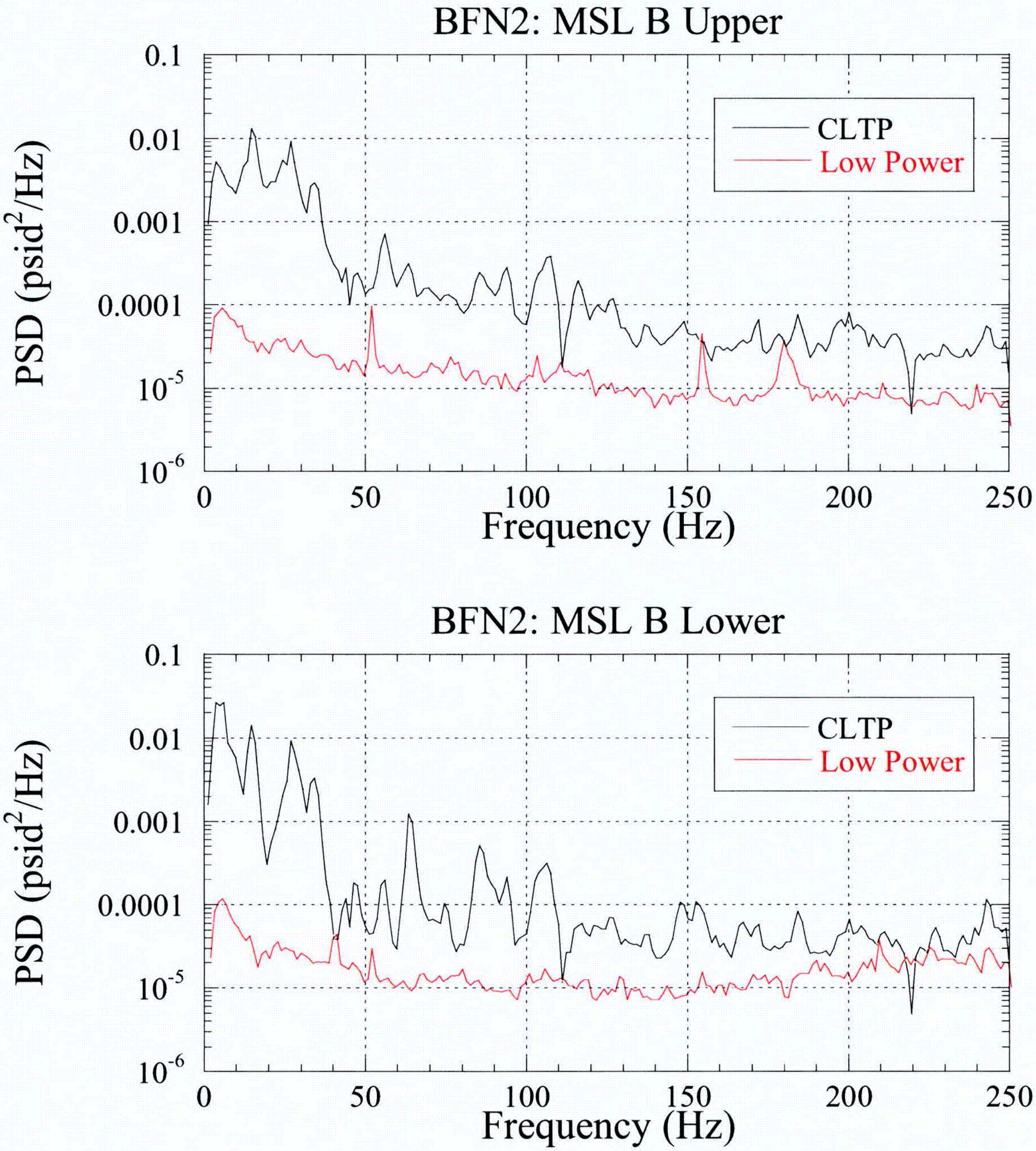

Figure 3.3. PSD comparison of pressure measurements on main steam line B at strain gage locations upper (top) and lower (bottom), for CLTP (black curves) and Low Power (red curves).

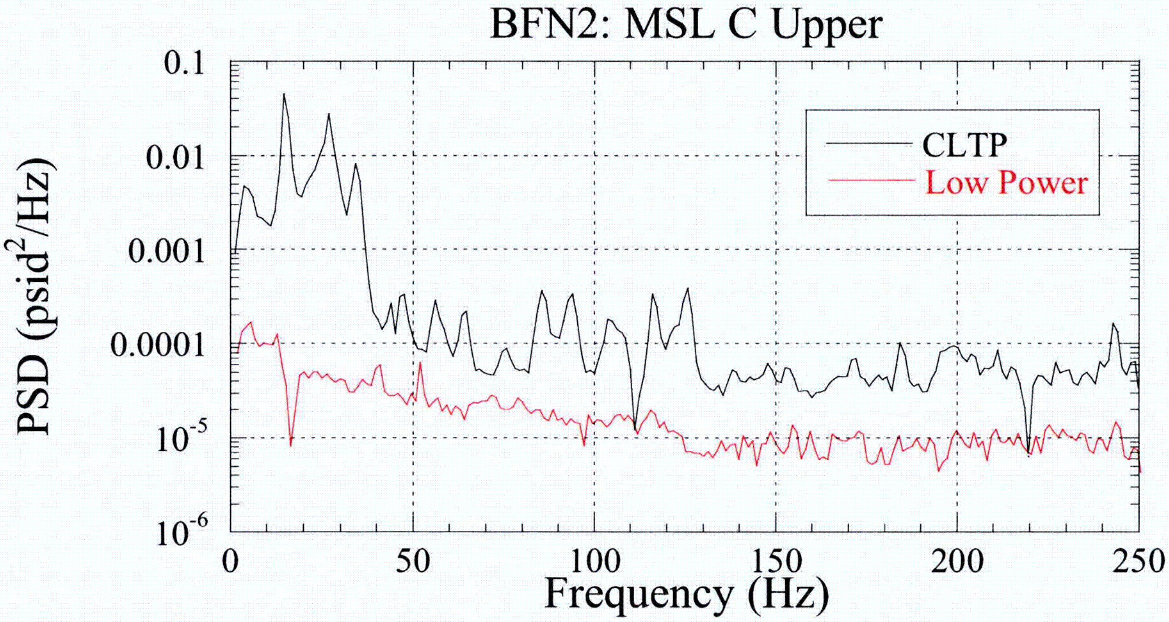

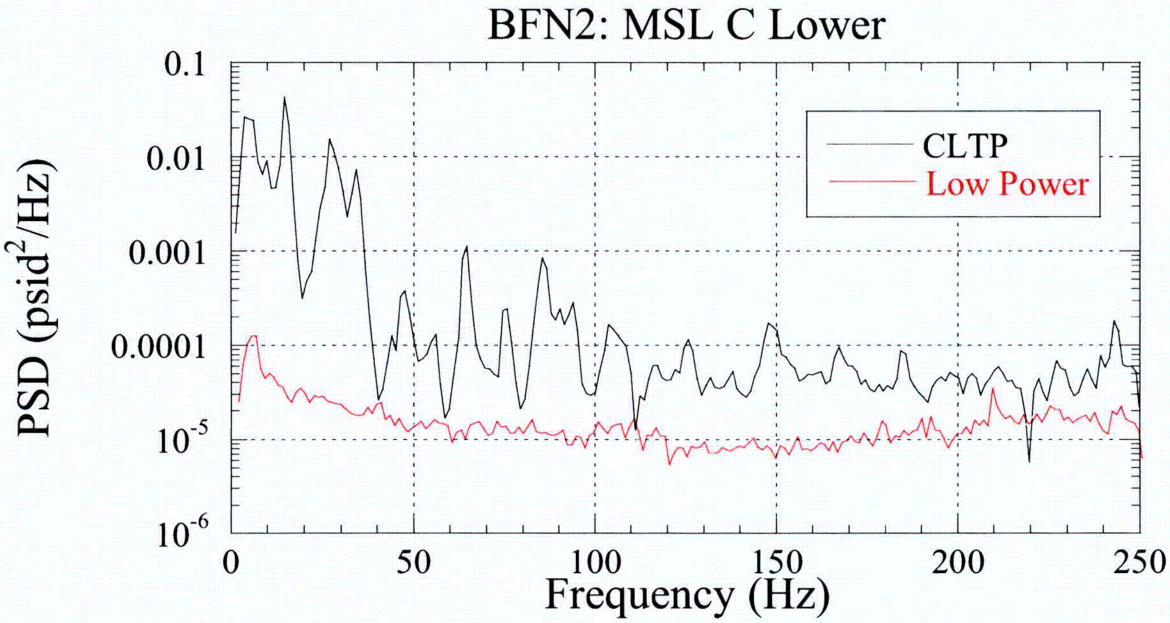

Figure 3.4. PSD comparison of pressure measurements on main steam line C at strain gage locations upper (top) and lower (bottom), for CLTP (black curves) and Low Power (red curves).

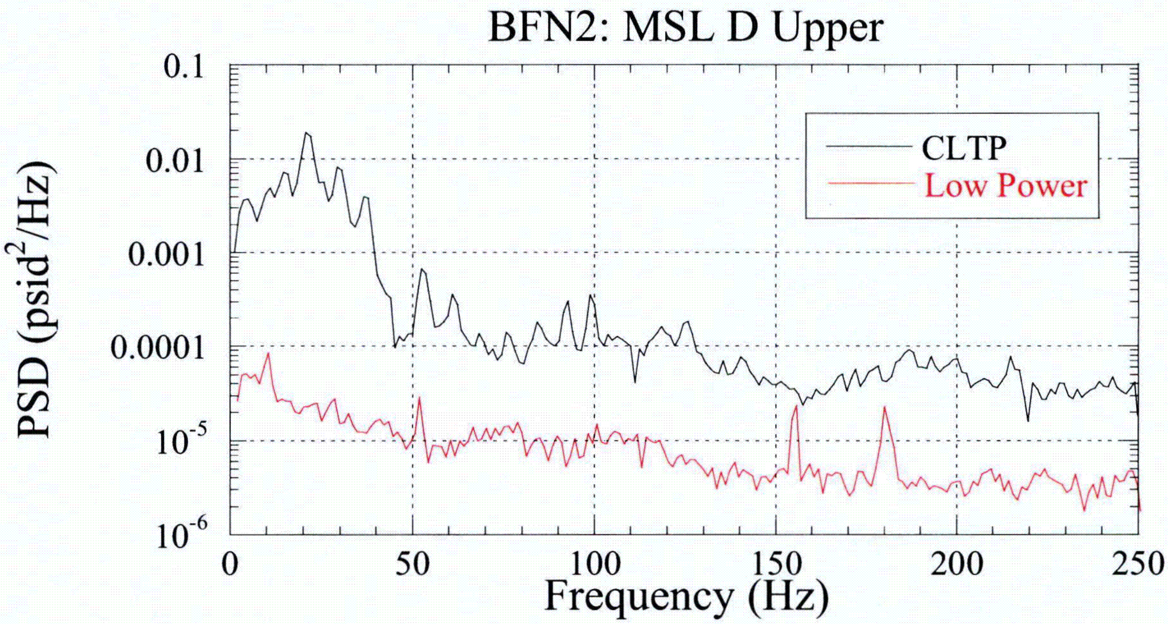

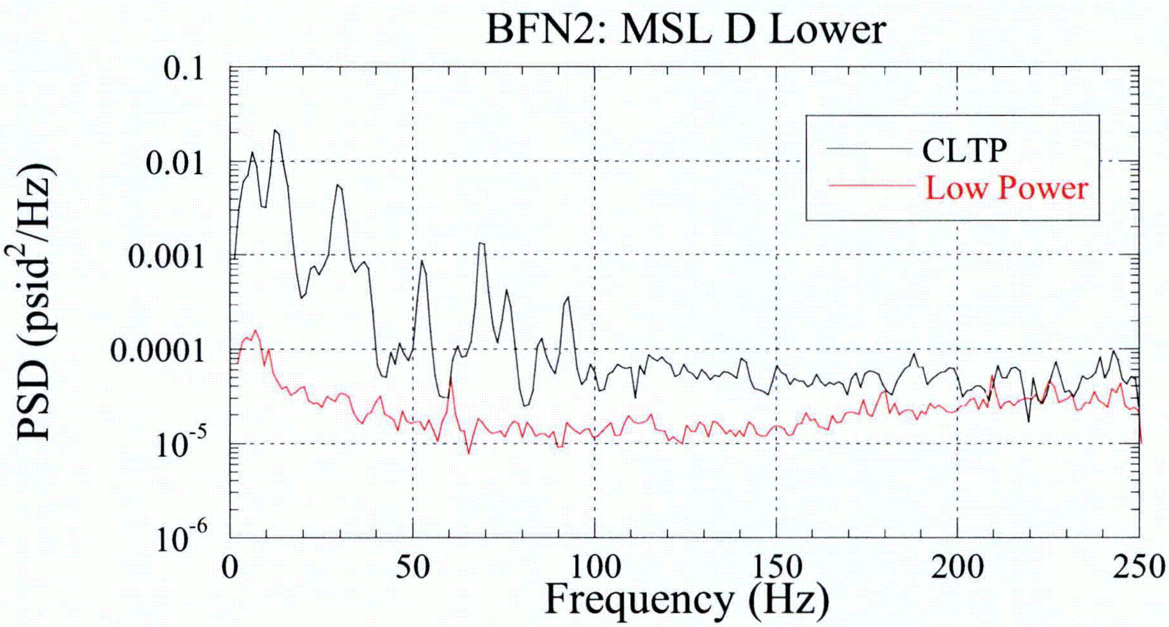

Figure 3.5. PSD comparison of pressure measurements on main steam line D at strain gage locations upper (top) and lower (bottom), for CLTP (black curves) and Low Power (red curves).

4. Results

The measured main steam line pressure data were used to drive the validated acoustic circuit methodology for the BFN2 steam dome coupled to the main steam lines to make a pressure load prediction on the BFN2 dryer. For the prediction shown here, the Low Power data are subtracted from the CLTP data using a formula similar to that shown for the removal of the electrical noise

$$P_R(\omega) = P_S(\omega)\left[1 - \left|\frac{P_L(\omega)}{P_S(\omega)}\right|\right]$$

where $P_R(\omega)$ is the CLTP signal $P_S(\omega)$ corrected for low power $P_L(\omega)$, computed as a function of frequency ω, and $|P_L(\omega)/P_S(\omega)|$ can be no larger than 0.5.

A low resolution load, developed at the nodal locations identified in Figures 4.1 to 4.4, produces the maximum differential and RMS pressure levels across the dryer as shown in Figure 4.5. PSDs of the peak loads on either side of the dryer are shown in Figure 4.6.

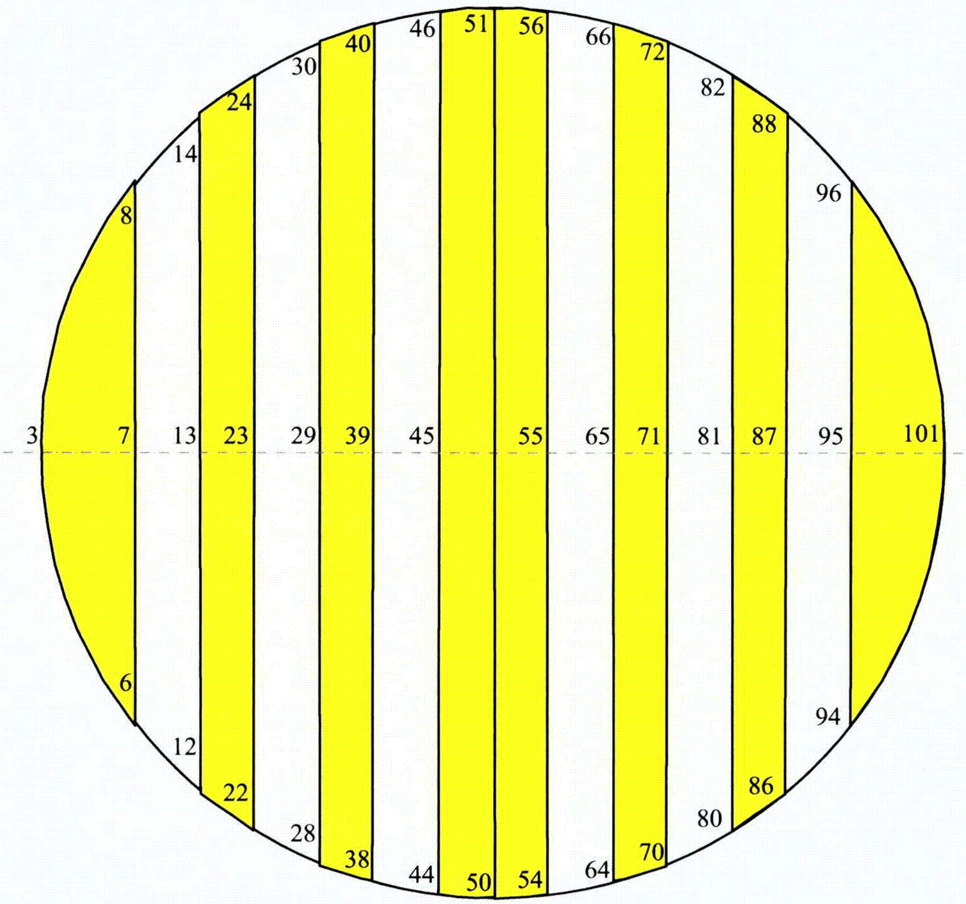

Figure 4.1. Bottom plates pressure node locations (low resolution), with pressures acting downward in the notation defined here.

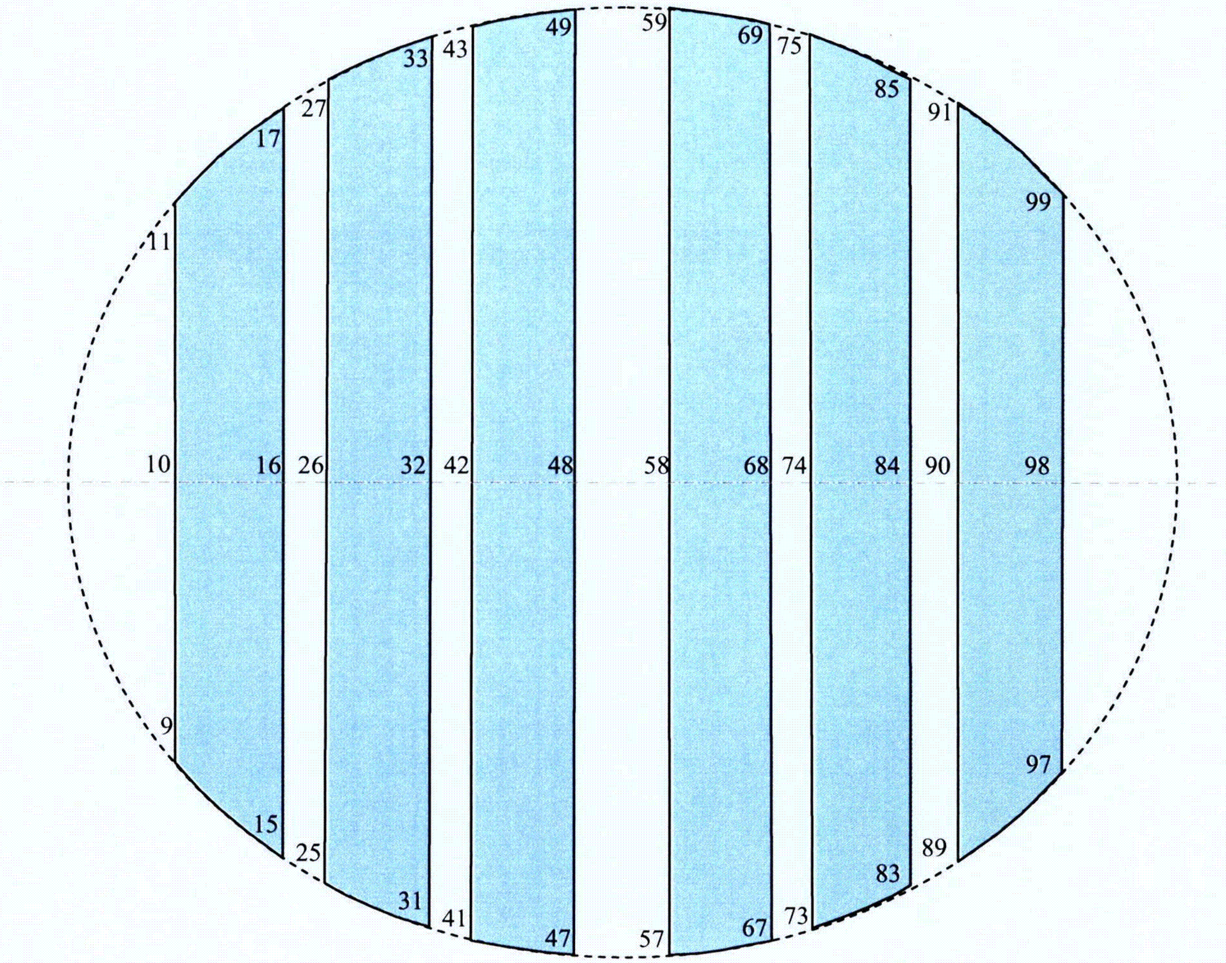

Figure 4.2. Top plates pressure node locations (low resolution), with pressures acting downward in the notation defined here.

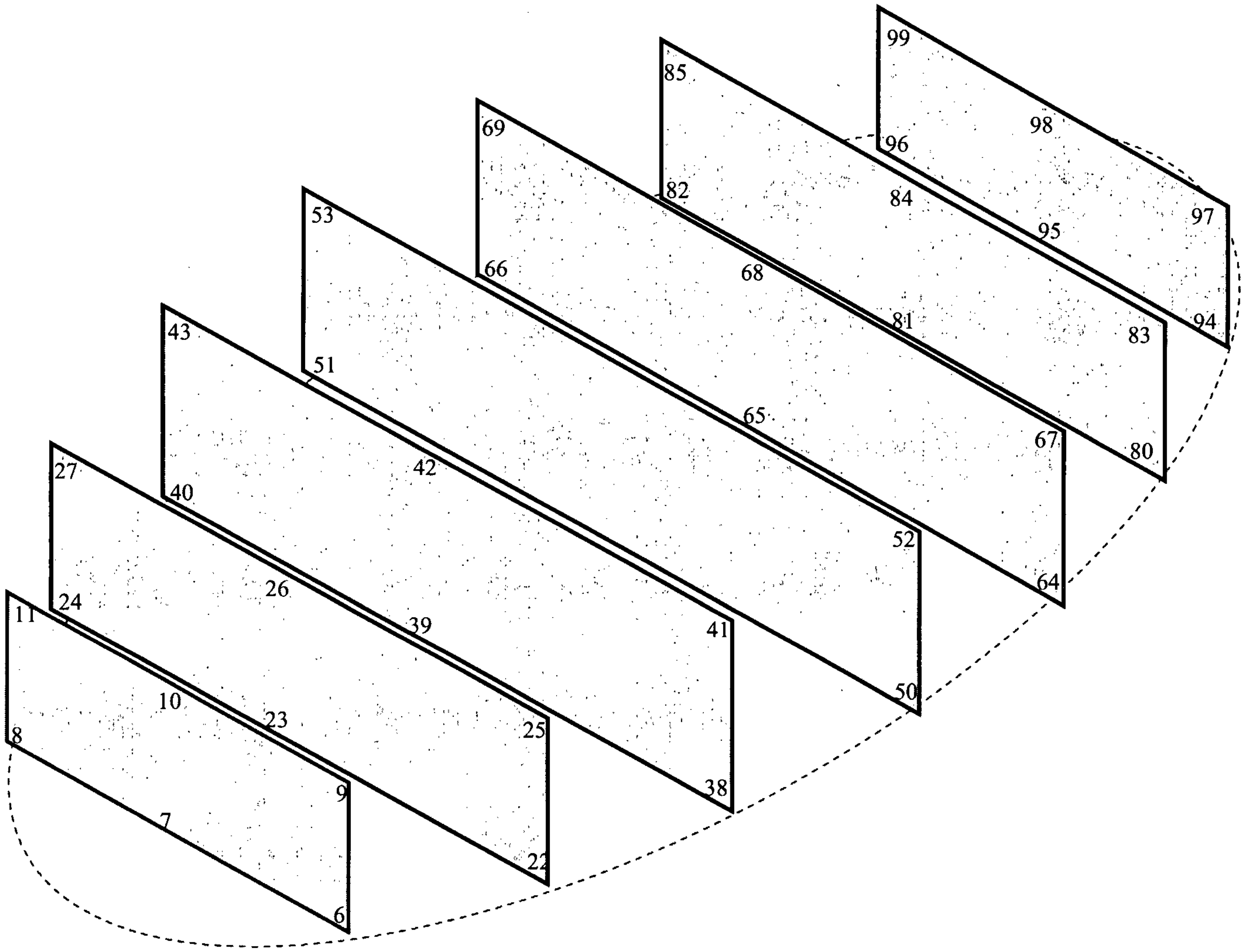

Figure 4.3. Vertical plates: Pressures acting left to right on panels 6-11, 22-27, 38-43, and 50-54; acting right to left on panels 64-69, 80-85, and 94-99 (low resolution).

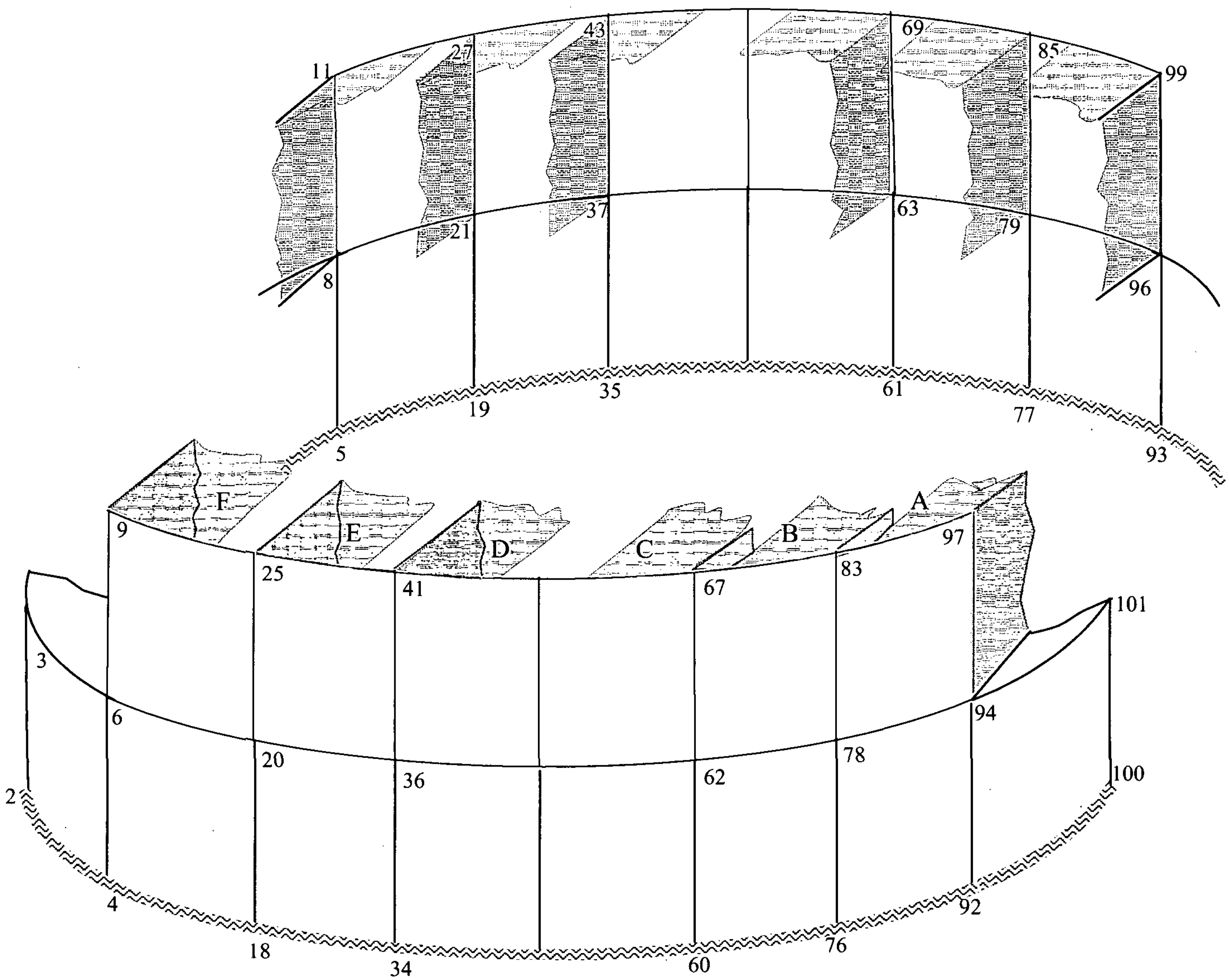

Figure 4.4. Skirt plates: Pressure acting outward on the outer dryer 0°/180° surfaces and the skirt (low resolution).

[[

(3)]]

Figure 4.5. Predicted CLTP loads on the low resolution grid identified in Figures 4.1 to 4.4, as developed by the Modified Bounding Pressure model, to 250 Hz. Low-numbered nodes are on the C-D side of the dryer, while high-numbered nodes are on the A-B side of the dryer.

[[

(3)]]

Figure 4.6. PSD of the maximum pressure loads predicted on the C-D side of the BFN2 dryer (top) and A-B side of the BFN2 dryer (bottom).

5. Uncertainty Analysis

The analysis of potential uncertainty occurring at BFN2 consists of several contributions, including the uncertainty from collecting data on the main steam lines at locations other than the locations on Quad Cities Unit 2 (QC2) and the uncertainty in the Modified Bounding Pressure model. QC2 dryer data at Original Licensed Thermal Power (OLTP) conditions were used to generate an uncertainty analysis of the Acoustic Circuit Methodology (ACM) [2] for BFN2.

The approach taken for bias and uncertainty is similar to that used by Vermont Yankee for power uprate [6]. In this analysis, six "averaged pressures" are examined on the instrumented replacement dryer at QC2: averaging pressure sensors P1, P2, and P3; P3, P5, and P6; P7, P8, and P9; P10, P11, and P12; P18 and P20; and P19 and P21. These pressure sensors were all on the outer bank hoods of the dryer, and the groups are comprised of sensors located vertically above or below each other.

Bias is computed by taking the difference between the measured and predicted RMS pressure values for the six "averaged pressures", and dividing the mean of this difference by the mean of the predicted RMS. RMS is computed by integrating the PSD across the frequency range of interest and taking the square root

$$\mathrm{BIAS} = \frac{\frac{1}{N}\sum(\mathrm{RMS}_{\mathrm{measured}} - \mathrm{RMS}_{\mathrm{predicted}})}{\frac{1}{N}\sum \mathrm{RMS}_{\mathrm{predicted}}} \tag{5.1}$$

where $\mathrm{RMS}_{\mathrm{measured}}$ is the RMS of the measured data and $\mathrm{RMS}_{\mathrm{predicted}}$ is the RMS of the predicted data. Summations are over the number of "averaged pressures", or N = 6.

Uncertainty is defined as the fraction computed by the standard deviation

$$\mathrm{UNCERTAINTY} = \frac{\sqrt{\frac{1}{N}\sum(\mathrm{RMS}_{\mathrm{measured}} - \mathrm{RMS}_{\mathrm{predicted}})^2}}{\frac{1}{N}\sum \mathrm{RMS}_{\mathrm{predicted}}} \tag{5.2}$$

ACM bias and uncertainty results are compiled for specified frequency ranges of interest, as directed by [7] and summarized in Table 5.1. Other random uncertainties, specific to BFN2, are summarized in Table 5.2 and are typically combined with the ACM results by SRSS methods to determine an overall uncertainty for BFN2.

Table 5.1. BFN2 bias and uncertainty for specified frequency intervals. A negative bias indicates that the ACM overpredicts the QC2 data in that interval.

[[

(3)]]

Table 5.2. Bias and uncertainty contributions to total uncertainty for BFN2 plant data.

[[

(3)]]

6. Conclusions

The C.D.I. acoustic circuit analysis, using full-scale measured data for BFN2:

a) [[[3]]]

b) Predicts that the loads on dryer components are largest for components nearest the main steam line inlets and decrease inward into the reactor vessel.

7. References

1. Continuum Dynamics, Inc. 2005. Methodology to Determine Unsteady Pressure Loading on Components in Reactor Steam Domes (Rev. 6). C.D.I. Report No. 04-09 (C.D.I. Proprietary).

2. Continuum Dynamics, Inc. 2007. Bounding Methodology to Predict Full Scale Steam Dryer Loads from In-Plant Measurements, with the Inclusion of a Low Frequency Hydrodynamic Contribution (Rev. 0). C.D.I. Report No. 07-09 (C.D.I. Proprietary).

3. Browns Ferry Unit 1 Drawings. 2006. Files: 729E229-1.tif, 729E229-2.tif, and 729E229-3.tif. BFN2 Email from G. Nelson dated 07 March 2006.

4. Structural Integrity Associates, Inc. 2006. Main Steam Line 100% CLTP Strain Data Transmission. SIA Letter Report No. GSZ-06-017.

5. Continuum Dynamics, Inc. 2007. Onset of Flow-Induced Vibration in the Main Steam Lines at Browns Ferry Unit 1: A Subscale Investigation of Standpipe Behavior (Rev. 0). C.D.I. Report No. 08-01 (C.D.I. Proprietary).

6. Communication from Enrico Betti. 2006. Excerpts from Entergy Calculation VYC-3001 (Rev. 3), EPU Steam Dryer Acceptance Criteria, Attachment I: VYNPS Steam Dryer Load Uncertainty (Proprietary).

7. NRC Request for Additional Information on the Hope Creek Generating Station, Extended Power Uprate. 2007. TAC No. MD3002. RAI No. 14.67.

8. Structural Integrity Associates, Inc. 2006. Evaluation of Browns Ferry Unit 2 Strain Gage Uncertainty and Pressure Conversion Factors (Rev. 0). SIA Calculation Package No. BFN-11Q-301.

9. Continuum Dynamics, Inc. 2005. Vermont Yankee Instrument Position Uncertainty. Letter Report Dated 01 August 2005.

10. Exelon Nuclear Generating LLC. 2005. An Assessment of the Effects of Uncertainty in the Application of Acoustic Circuit Model Predictions to the Calculation of Stresses in the Replacement Quad Cities Units 1 and 2 Steam Dryers (Revision 0). Document No. AM-21005-008.

11. Continuum Dynamics, Inc. 2007. Finite Element Modeling Bias and Uncertainty Estimates Derived from the Hope Creek Unit 2 Dryer Shaker Test (Rev. 0). C.D.I. Report No. 07-27 (C.D.I. Proprietary).

12. NRC Request for Additional Information on the Hope Creek Generating Station, Extended Power Uprate. 2007. RAI No. 14.79.

13. NRC Request for Additional Information on the Hope Creek Generating Station, Extended Power Uprate. 2007. RAI No. 14.110.